Sequence-specific interaction of Hoescht 33258 with the minor groove of an adenine-tract DNA duplex studied in solution by ^{1}H NMR spectroscopy

Mark S.Searle* and Kevin J.Embrey[1]
Peter MacCallum Cancer Institute NMR Facility and [1]Department of Pharmaceutical Chemistry, Victorian College of Pharmacy, Parkville, Australia

Received April 12, 1990; Accepted May 18, 1990

ABSTRACT

The interaction of Hoechst 33258 with the minor groove of the adenine-tract DNA duplex d(CTTTTGCAAAAG)$_2$ has been studied in both D_2O and H_2O solutions by 1D and 2D ^{1}H NMR spectroscopy. Thirty-one nuclear Overhauser effects between drug and nucleotide protons within the minor groove of the duplex, together with ring-current induced perturbations to the chemical shifts of basepair and deoxyribose protons, define the position and orientation of the bound dye molecules. Two drug molecules bind cooperatively and in symmetry related orientations at the centre of the 5′-TTTT and 5′-AAAA sequences with the binding interactions spanning only the four A-T basepairs. The positively charged N-methylpiperazine moieties point towards the centre of the duplex while the phenol groups are disposed towards the 3′-ends of the sequence. Resonance averaging is apparent for both the D2/D6 and D3/D5 phenol protons and D2‴/D6‴ and D3‴/D5‴ of the N-methylpiperazine ring and is consistent with these groups being involved in rapid rotation or ring-flipping motions in the bound state. Interstrand NOEs between adenine H2s and deoxyribose H1′ are consistent with a high degree of propeller twisting of the A-T basepairs at the binding site of the aromatic benzimidazole and phenol rings of Hoechst. The data imply that the minor groove is particularly narrow with many contacts between the complementary curved surfaces of the drug and DNA indicating that strong van der Waals interactions, involving the floor and the walls of the minor groove, stabilize the complex. In our model the NH groups of the benzimidazole rings are positioned to make a pair of bifurcated hydrogen bonds with the adenine N3 and thymine O2 on the floor of the minor groove.

INTRODUCTION

Hoechst 33258 (Figure 1) binds to the minor groove of right-handed double-stranded DNA rich in A-T basepairs (1). It is a synthetic compound containing two linked benzimidazole rings with phenol and N-methyl-piperazine moieties attached at either end of the structure. Its interaction with DNA has been well studied and has been shown to possess both a low-level tight-binding affinity (binding constant 10^6-10^7 M^{-1}) and a high-level low-affinity binding component (binding constant 10^4-10^5 M^{-1}) that are differentiated by their fluorescence characteristics (2, 3). Hoechst has found widespread use as a fluorescent cytological DNA stain but is also active as an anthelmintic agent (4, 5) and has demonstrated activity against intraperitoneally implanted L1210 and P388 leukemias in mice (6). Its mechanism of action in murine cell lines appears to involve an inhibition of chromosomal DNA condensation (9, 10). Footprinting studies with methidiumpropyl EDTA-Fe(II) (9) and the observation of double-stranded breaks induced by ^{125}I-labelled Hoechst (10, 11) reveal that a sequence of four consecutive A-T basepairs is a primary requisite for strong binding to DNA. Thus, the groove binding agents Hoechst, netropsin and distamycin, all of which are formed from a repeating structural motif, share common recognition properties which appear to be related to the conformation of DNA in A-T rich regions.

Recently a number of crystal structures of Hoechst 33258 complexed to oligonucleotide duplexes have been reported. Two of these structures describe the interaction of Hoechst with the sequence d(CGCGAATTCGCG)$_2$ (12, 13), the third with d(CGCGATATCGCG)$_2$ (14). In all three structures the Hoechst dye interacts principally with the central A-T basepairs although in the structures of Pjura et al. (12) and Carrondo et al. (14) it is displaced such that binding encompasses the ATTC and GATA sequences, respectively. The Hoechst molecules in these two structures have opposite orientations but in each case the charged N-methylpiperazine rings extend into the GC region flanking the A-T basepairs where the groove is wider and more readily able to accommodate this bulky portion of the molecule. Such apparent GC selectivity is not found by Teng et al. (13) who report that Hoechst binds in the middle of the AATT sequence. In all three structures the binding interaction is the result of hydrogen bonding, electrostatic and van der Waals contacts between the Hoechst molecule and the narrow minor

* To whom correspondence should be addressed at Peter MacCallum Cancer Institute NMR Facility, Victorian College of Pharmacy, 381 Royal Parade, Parkville, Victoria 3052, Australia

groove. In particular the complex is stabilised by hydrogen bonds from the NH groups on the benzimidazole rings (see Figure 1) to the thymine O2 and adenine N3 in the minor groove. Close van der Waals contacts are observed between the drug and adenine H2s on the floor of the groove and the deoxyribose O4′ forming the walls of the binding site.

Our efforts have been directed towards obtaining valuable structural information on the interaction and sequence binding preferences of Hoechst 33258 with DNA in solution to complement the crystalline data already reported. Here we describe NMR studies of the complex formed between the self-complementary dodecanucleotide duplex d(CTTTTGCAA-AAG)$_2$ and the Hoechst dye. This DNA sequence contains runs of adenine and thymine bases which have been shown to be high-affinity binding sites for Hoechst in natural DNA (13, 14). The sequence contains two possible binding sites, and indeed we find that two Hoechst molecules interact with the DNA duplex in symmetry related orientations at the 5′-TTTT and 5′-AAAA sites. Structural details of the complex have been established from 1D and 2D NOE experiments which define both the position and orientation of the Hoechst molecules within the A-T tracts. Our findings are compared with the crystal structure data previously reported and are consistent with Hoechst binding at the centre of the tracts of A-T basepairs.

MATERIALS AND METHODS

The dodecanucleotide undecaphospate d(CTTTTGCAAAAG) was synthesized 'trityl-off' using automated solid-phase phosphoramidite chemistry on an Applied Biosystems 381A DNA synthesizer. After cleavage and deprotection the oligonucleotide was purified using a combination of anion exchange and reverse-phase chromatography using Pharmacia Mono Q and Pro RPC columns, respectively. In the final step the oligonucleotide was converted from the triethylammonium salt to the sodium form by passage down a Mono S cation exchange column and was judged to be >95% pure by analytical HPLC and ^{1}H NMR. After repeated lyophilization from D_2O solution at pH 7.0, containing 10 mM sodium phosphate and 50 mM sodium chloride, the sample was dissolved in 0.55 mL of 99.96% D_2O (Aldrich) for NMR studies. Hoechst 33258 was obtained from Aldrich and was used without purification. The Hoechst/DNA complex was generated by adding small aliquots of a 10 mM stock solution of Hoechst in D_2O to a 2 mM solution of the oligonucleotide duplex. The stoichiometry of the complex was monitored by ^{1}H NMR.

^{1}H NMR spectra were collected at 400 MHz on a Varian VXR400 wide-bore spectrometer and the data processed on a Sun 3/50 data station using Varian software. Pure absorption phase-sensitive COSY and NOESY spectra were acquired using the hypercomplex method of data collection (15, 16) with the carrier frequency placed at the centre of the spectrum at the frequency of the HDO solvent resonance. The latter was suppressed using low-power selective irradiation during the relaxation delay of 1.0 s. A spectral width of 4000 Hz was employed with 2D spectra being acquired as 1024 points in t_2 for $2\times300-400$ t_1 increments and zero-filled to 1024 points in t_1 prior to Fourier transformation. NOESY data sets collected at 50, 100 and 200 ms were apodized with shifted sinebell window functions in t_2 and a mild gaussian window in t_1. The COSY data is presented in the absolute value mode for which unshifted sinebell window functions were applied during data processing. 1D spectra collected in 90% H_2O/ 10% D_2O solution employed a 10,000 Hz spectral width with a 1−1 binomial read pulse producing on-resonance suppression of the solvent peak (17, 18). An offset of 3000 Hz produced maximum signal intensity at the centre of the imino proton region of the spectrum. 1D NOE difference spectra recorded in 90% H_2O were similarly obtained using the binomial solvent suppression sequence and by subtracting free-induction decays obtained from on and off resonance selective irradiation for 300 ms prior to acquisition. A total of 1024 transients were collected in the interleaved mode cycling in blocks of 16 transients at each irradiation frequency with a relaxation delay of 1.5 s per transient.

Nucleotide residues are numbered sequentially from the 5′-end of the dodecamer, viz., d(C1-T2-T3-T4-T5-G6-C7-A8-A9-A10-A11-G12). Drug protons are identified in the text and figures as D, for example D4′, while those of the DNA are labelled H and according to residue number, for example, C1H1′.

RESULTS

Symmetry of the complex and site of drug binding

Illustrated in Figure 1 are portions of the 1D ^{1}H NMR spectra of d(CTTTTGCAAAAG)$_2$ recorded at the ligand concentrations indicated. In the presence of one equivalent of Hoechst per duplex we observe a complex spectrum with resonances attributable to the ligand-free DNA together with those of a bound form. Several new resonances appear in previously unoccupied spectral windows, for example, two signals become apparent between 6.0−6.5 ppm which were later assigned to T5H6 and T2H1′ in the complexed form of the duplex. The absence of signal averaging confirms that the free and complexed forms of the DNA are in slow exchange with each other under these conditions. Addition of further quantities of drug results in a reduction in the intensity of the signals of the free DNA until at a ratio of 2 Hoechst molecules per DNA duplex we observe a single species in solution which retains the dyad symmetry observed for the DNA alone. This is best illustrated by the effects of drug concentration on the thymine methyl resonances between 1.0−1.5 ppm. In the 2:1 complex four methyl resonances are clearly resolved while at a 1:1 ratio only resonances from the 2:1 complex and the free DNA are detected. This observation leads us to conclude that two Hoechst molecules bind cooperatively to d(CTTTTGCAAAAG)$_2$ in symmetry related orientations. No evidence is found for any detectable quantity of an intermediate 1:1 complex. In the NOESY spectrum of the mixture of free and complexed DNA a large number of chemical exchange cross-peaks are observed between DNA resonances in the two dyad symmetrical forms, as illustrated for the aromatic region of the spectrum in Figure 2A. At 25°C these cross-peaks have intensities significantly larger than those corresponding to NOE interactions, however, when the experiment is repeated at 10°C their intensities are considerably reduced indicating that although the two species are freely interconverting at 25°C the rate is much slower at the lower temperature, estimated from a series of 1D and 2D magnetization transfer experiments to be $<10\ s^{-1}$ at 10°C (data not shown). The chemical exchange data provide a convenient method of transferring resonance assignments between the free and bound forms of the duplex although conventional methodologies were used to check these assignments for the fully complexed DNA, as described below. In a number of cases chemical shift differences of ~1.0 ppm are evident between the free and bound forms of the duplex. In

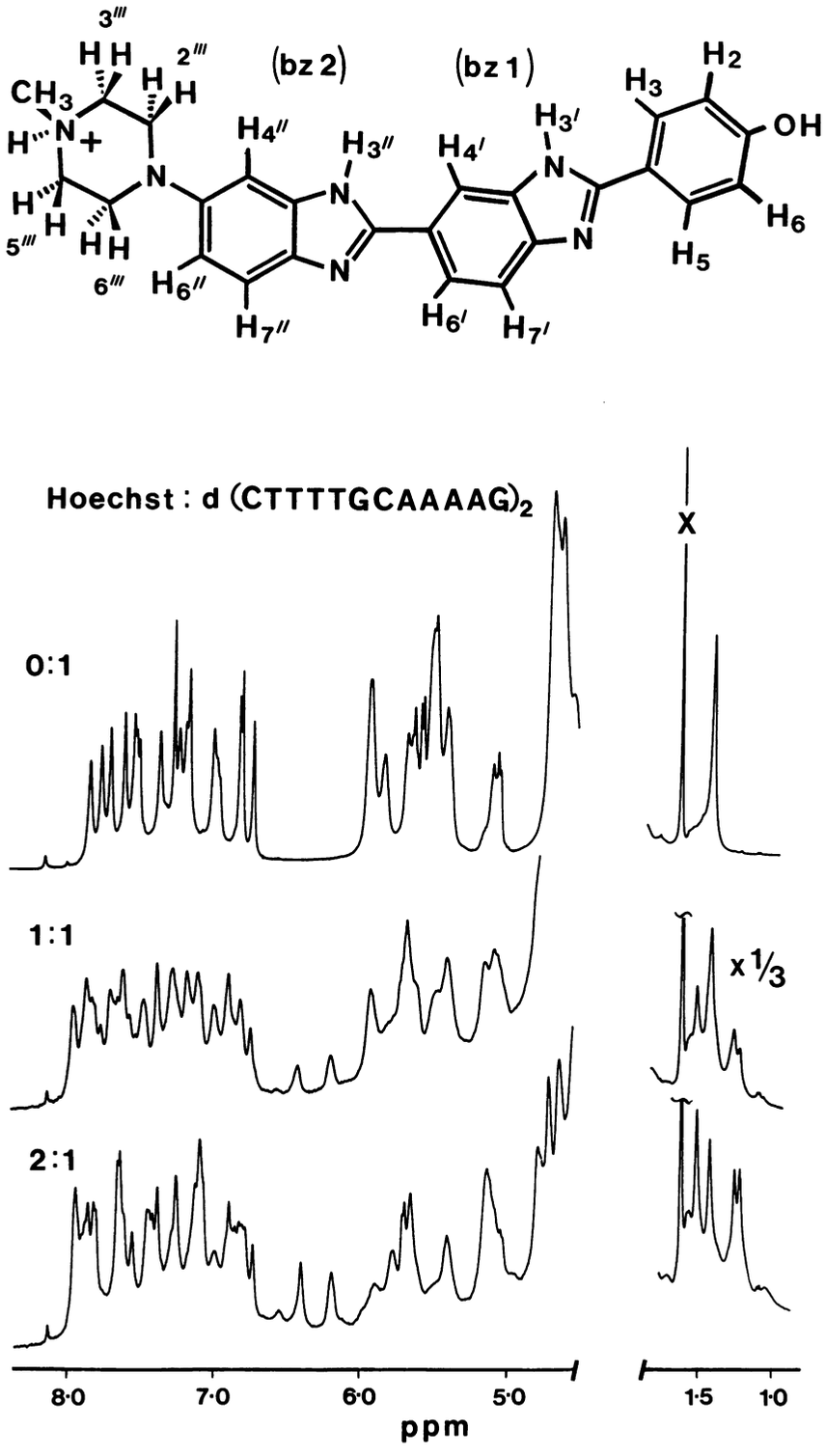

Figure 1. Structure of Hoechst 33258 and proton labelling scheme (A). Portions of the 1D ^{1}H NMR spectra of d(CTTTTGCAAAAG)$_2$ recorded at 10°C at the various ratios of Hoechst indicated (B). X marks the position of an impurity peak due sodium acetate.

particular, T3H1′, T4H1′, T5H1′, A11H1′ and also G12H1′ experience large upfield shifts of between 0.78 and 1.13 ppm, while A9H2, A10H2 and A11H2 experience large downfield shifts of between 0.60 and 0.85 ppm. Perturbations of this magnitude to the chemical shifts of these resonances are consistent with the drug molecules binding in the minor groove within the adenine tracts. In contrast, generally small chemical shift changes are observed for the base H6/H8 and CH_3 which are found in the major groove, with the largest effect being an upfield shift of 0.6 ppm for T5H6. The chemical shift changes for some of the assigned resonances versus position in the sequence are presented in Figure 2B.

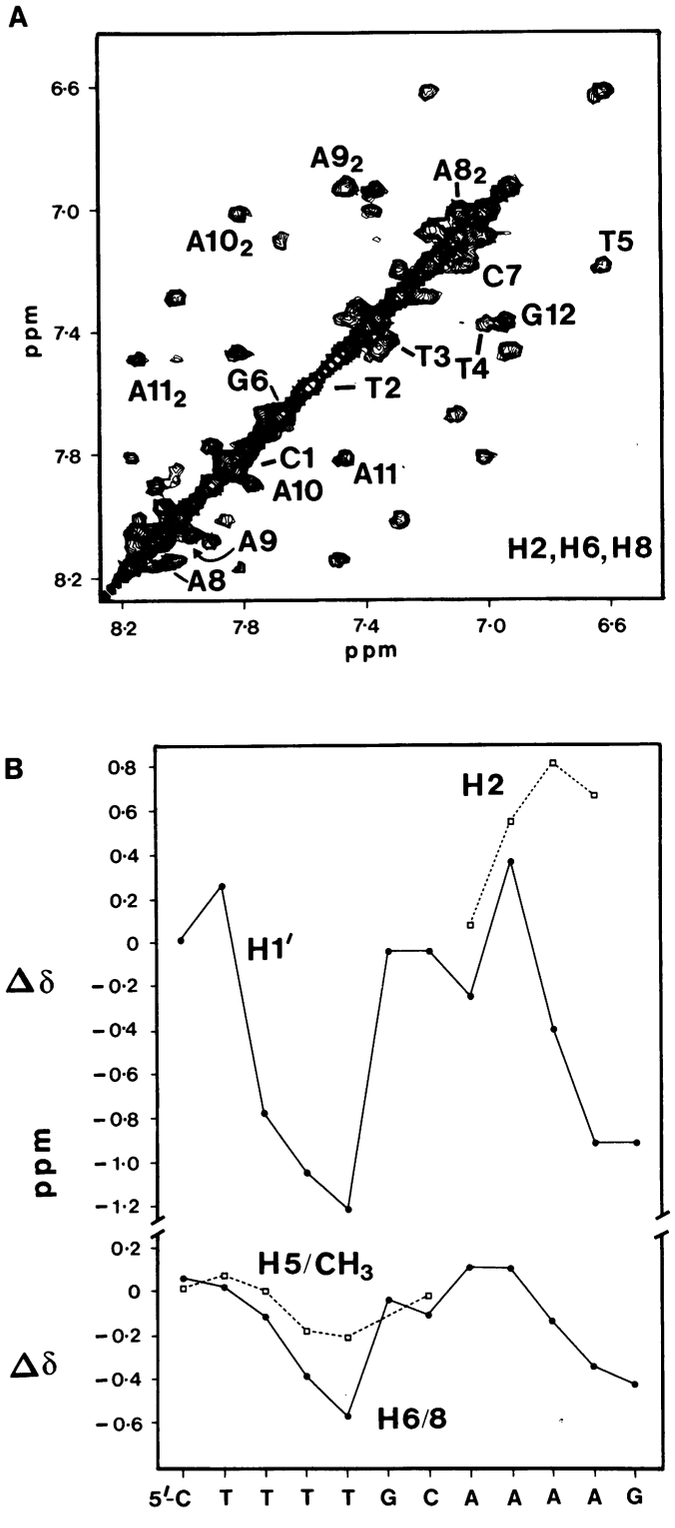

Figure 2. Aromatic portion of the 2D phase-sensitive NOESY (Chemical Exchange) spectrum of the 1:1 Hoechst:DNA mixture recorded at 25°C, mixing time 200ms (A). Chemical exchange cross-peaks between protons of the free DNA and the 2:1 Hoechst:DNA complex are highlighted. Below the diagonal the base H6 and H8 cross-peaks are identified, while those of the adenine H2 resonances are highlighted in the upper portion of the figure and are labelled with subscript '2'. Plots of chemical shift differences Δδ between free and complexed forms of d(CTTTTGCAAAAG)$_2$ recorded at 25°C are illustrated in (B). Perturbations to the resonances of base H6/H8, H5/CH3 (major groove) and H1′, H2 (minor groove) are highlighted. Positive shift differences correspond to resonances that move downfield upon binding of Hoechst, negative differences correspond to upfield complexation shifts.

DNA ^{1}H resonance assignments

A detailed picture of the interaction of Hoechst 33258 with d(CTTTTGCAAAAG)$_2$ follows from the assignment of the ^{1}H NMR spectrum of the fully complexed DNA from an analysis of 1D and 2D NMR data (20–22). Firstly, J-coupling interactions, manifested in COSY spectra, permit the deoxyribose spin-systems to be delineated and the cytosine H5-H6 and thymine CH_3-H6 correlations to be identified. Secondly, through-space internucleotide interactions observed in NOESY spectra permit base and deoxyribose spin-systems to be assigned sequence-specifically. The NOE data is also used to complement the COSY data to confirm and extend the assignments of the deoxyribose spin-systems. The 200ms NOESY spectrum of the complex is illustrated in Figure 3A. Highlighted are the regions of the spectrum containing the inter and intranucleotide connectivities H6/H8(i)-H1′(i)-H6/H8(i+1) and H6/H8(i)-H2′/2″(i)-H6/H8(i+1) which appear in expanded form in Figure 4A and 4B, respectively. Also illustrated in Figure 4B are the correlations H6(i)-CH_3(i+1)-H6(i+1) identified along the C1-T5 stretch of the sequence. The C1H6 resonance provides the starting point and is assigned from the lowest field of the two cytosine H5-H6 COSY cross-peaks apparent in the aromatic region of the COSY spectrum illustrated in Figure 3B. From the NOESY data of Figure 4A the first route via base and deoxyribose H1′ is highlighted with intranucleotide cross-peaks being labelled according to position in the sequence. The procedure begins with the C1H6-C1H1′ cross-peak (labelled C1) and proceeds to C1H1′-T2H6 and onward along the sequence. In Figure 4B sequential correlations between the base protons and deoxyribose H2′/2″ are also fully resolved and confirm the base proton resonance assignments obtained using the first of the sequential pathways and the chemical exchange data. The chemical exchange assignments of the adenine H2 resonances (illustrated in Figure 2A) are confirmed by the observation of a number of inter and intrastrand cross-peaks in the NOESY spectrum of the fully complexed DNA. For example, H2(i)-H2(i+1) sequential NOEs are observed for all steps along the adenine-tract (data not shown) as well as interstrand interactions between adenine H2 and the deoxyribose H1′ of the complementary nucleotide to the 5′-neighbouring residue. Such interactions are readily identified for A11H2-T3H1′, A10H2-T4H1′ and A9H2-T5H1′ (see Figure 4A) and are indicative of highly propeller twisted A-T basepairs close to the drug binding site.

Imino proton resonance assignments

The low field portion of the ^{1}H NMR spectrum of the complex recorded in 90% H_2O/ 10% D_2O solution at 10°C is illustrated in Figure 5 along with a set of NOE difference spectra obtained from selective irradiation of each individual imino proton resonances. Many of these signals are shifted downfield upon complexation with particularly large perturbations of ~1.0 ppm observed for T2 and T3. The assignment of each thymine H3 resonance is based upon the observation of intense NOEs to the H2 of the basepaired adenine. For example, in Figure 5 NOEs are observed from the overlapping T2H3 and T3H3 resonances to the previously assigned A10 and A11H2. Similar effects are observed from T4H3 to A9H2 and from T5H3 to A8H2. In a number of cases, where resonances are sufficiently well separated to allow selective irradiation without spill-over effects to neighbouring resonances, NOEs between the imino protons of sequentially neighbouring basepairs substantiate these assignments. In addition irradiating the G12H1 and G6H1

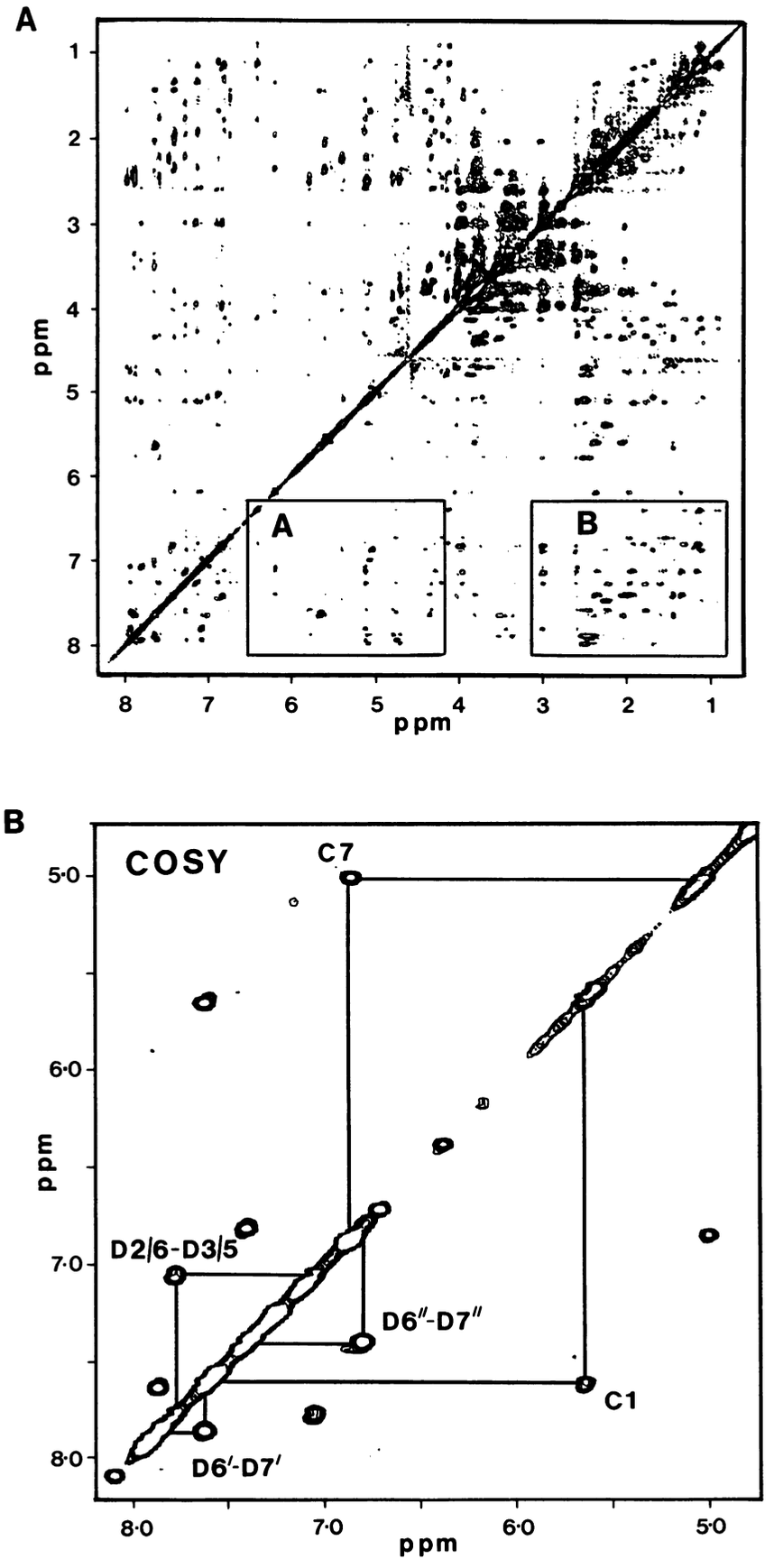

Figure 3. Contour plot of the phase-sensitive NOESY spectrum of the 2:1 Hoechst:DNA complex recorded at 10°C, mixing time 200ms (A). The boxed regions appear in expanded form as (A) and (B) in Figure 4. In (B) the 5.0−8.0 ppm region of the 10°C COSY spectrum of the 2:1 complex is illustrated. Cross-peaks corresponding to cytosine H5-H6 couplings are identified for C1 and C7 together with three additional correlations assosciated with the bound Hoechst molecules, as labelled.

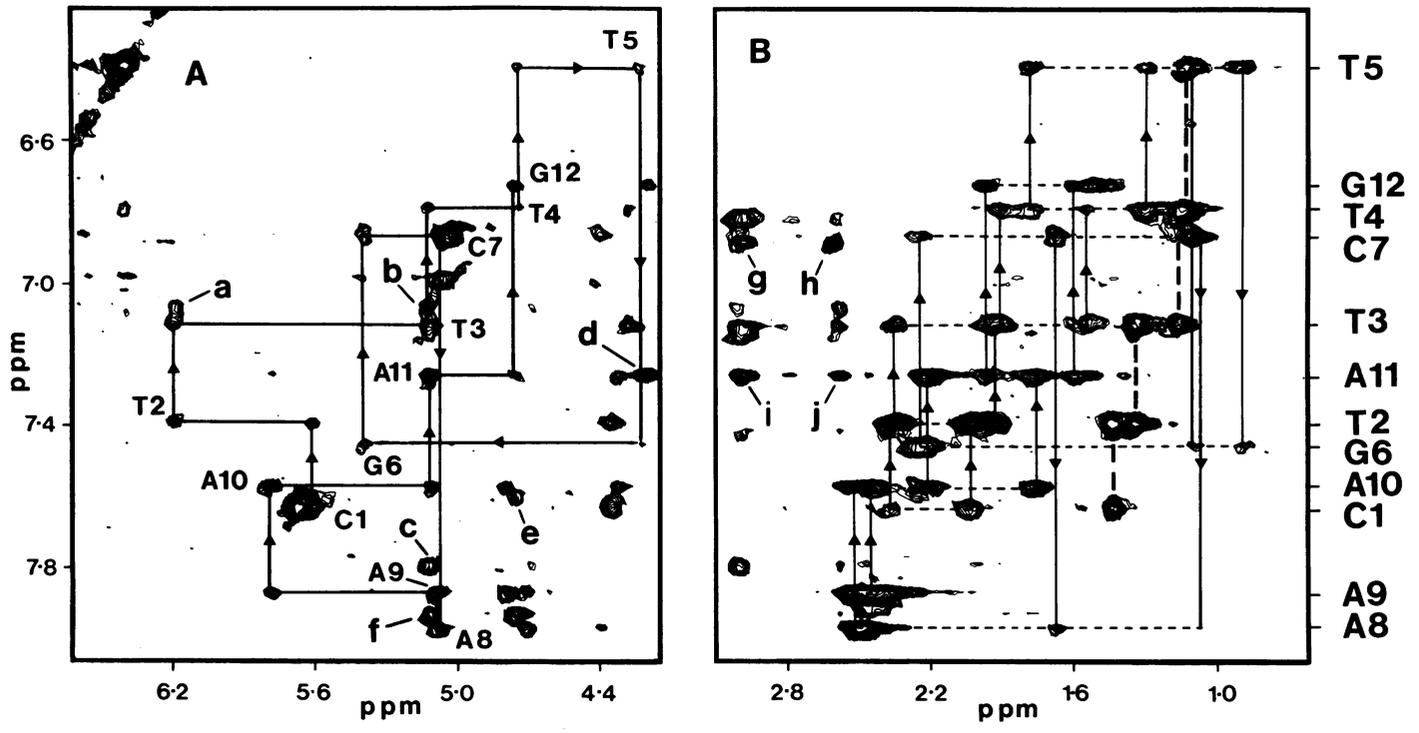

Figure 4. Portions of the phase-sensitive NOESY spectrum (mixing time 200ms) of the 2:1 Hoechst:DNA complex recorded at 10°C. In (A) sequential connectivities via base H6/H8 and deoxyribose H1′ are highlighted with labels identifying the intranucleotide cross-peaks for each residue. The base proton H6 or H8 assignments are indicated to the right-hand side of the figure. The cross-peaks labelled (a)−(f) are assigned as follows: (a) D2/6-T2H1′, (b) D2/6-T3H1′, (c) D3/5-T3H1′, (d) A9H2-T5H1′, (e) A10H2-T4H1′ and (f) A11H2-T3H1′. In (B) sequential correlations are traced between base H6/H8 and the intervening deoxyribose H2′/2″. Vertical lines connect correlations from a particular base proton to the sugar protons of the 5′-neighbouring residue. For example, NOEs are identified from C1H6 to T2H2′/2″. Also illustrated in bold broken lines are sequential correlations between base H6 and thymine CH_3 along the C1-T5 stretch of the sequence. The cross-peaks labelled (g)-(j) are assigned as follows: (g) D2‴/6‴ and/or D3‴/5‴-A8H2, (h) N-Me-A8H2, (i) D2‴/6‴ and/or D3‴/5‴-A9H2, (j) N-Me-A9H2.

identifies the slowly exchanging NH_2 protons of the basepaired cytosine residues.

Hoechst ^{1}H resonance assignments in the complex

The aromatic portion of the COSY spectrum of the complex, illustrated in Figure 3B, contains three cross-peaks, in addition to those of the two cytosine H5-H6, which originate from the proton pairs D2/6-D3/5, D6′-D7′ and D6″-D7″ of the bound Hoechst molecule. These cross-peaks are assigned specifically on the basis of intramolecular NOE effects observed in both D_2O and 90% H_2O solutions. Firstly, the methylene protons of the N-methylpiperazine rings are assigned on the basis of NOE effects from the N-methyl resonance, readily identified at 2.59 ppm. In the 100 ms NOESY spectrum (data not shown) strong correlations are identified to the D3‴/D5‴ protons located at 2.99/3.42 ppm, which in turn are close to those of D2‴/D6‴ at 2.99/3.95 ppm. Strong correlations are observed in D_2O NOESY spectra between D2‴/D6‴ of the N-methylpiperazine ring and the scalar coupled D6″ and D7″ (at 6.84 and 7.42 ppm, respectively), with the former interaction being strongest in the 100ms spectrum. Also observed are NOEs from these methylene protons to a singlet resonance, not previously assigned to a DNA base proton, which we attribute to D4″ on the benzimidazole ring (bz 2). In 90% H_2O solution the exchangeable proton resonances of D3′ (bz 1) and D3″ (bz 2) are readily identified at 11.27 and 11.08 ppm approximately 1.5 ppm upfield of the DNA imino proton resonances (12.5−14.5 ppm). The 1D NOE difference spectrum obtained by selectively irradiating the resonances at 11.27 ppm (see Figure 5) reveals strong NOE effects to a pair of scalar coupled proton resonances at 7.79 and 7.06 ppm previously identified in the COSY spectrum of Figure 3B. We attribute these latter resonances to the phenol D3/5 and D2/6 protons, respectively, and the former resonance at 11.27 ppm to the benzimidazole D3′. Thus, we identify the resonance at 11.08 ppm as that of D3″. This latter assignment is confirmed by the observation of NOE effects from both D3′ and D3″ to a previously unidentified resonance at 7.94 ppm, which we attribute to D4′, and from D3″ to the previously assigned D4″.

DNA and drug chemical shift values are presented in Table I.

Intermolecular interactions

The ^{1}H assignments for both drug and DNA resonances provide the basis for a detailed study of the interaction between Hoechst 33258 and d(CTTTTGCAAAAG)$_2$. Thirty-one NOEs are observed between drug and nucleotide protons and these are presented in Table II. Many of the relevant cross-peaks are highlighted in the 2D and 1D spectra of Figures 4 and 5, respectively. These interactions place considerable constraints on the structure of the complex and allow us to distinguish between the two possible orientations of the drug molecules when bound to d(CTTTTGCAAAAG)$_2$. Interactions are observed along the full length of the adenine-tract as represented schematically in Figure 6A. At one end of the binding site we observe, for example, strong NOEs between the drug phenol protons D2/6

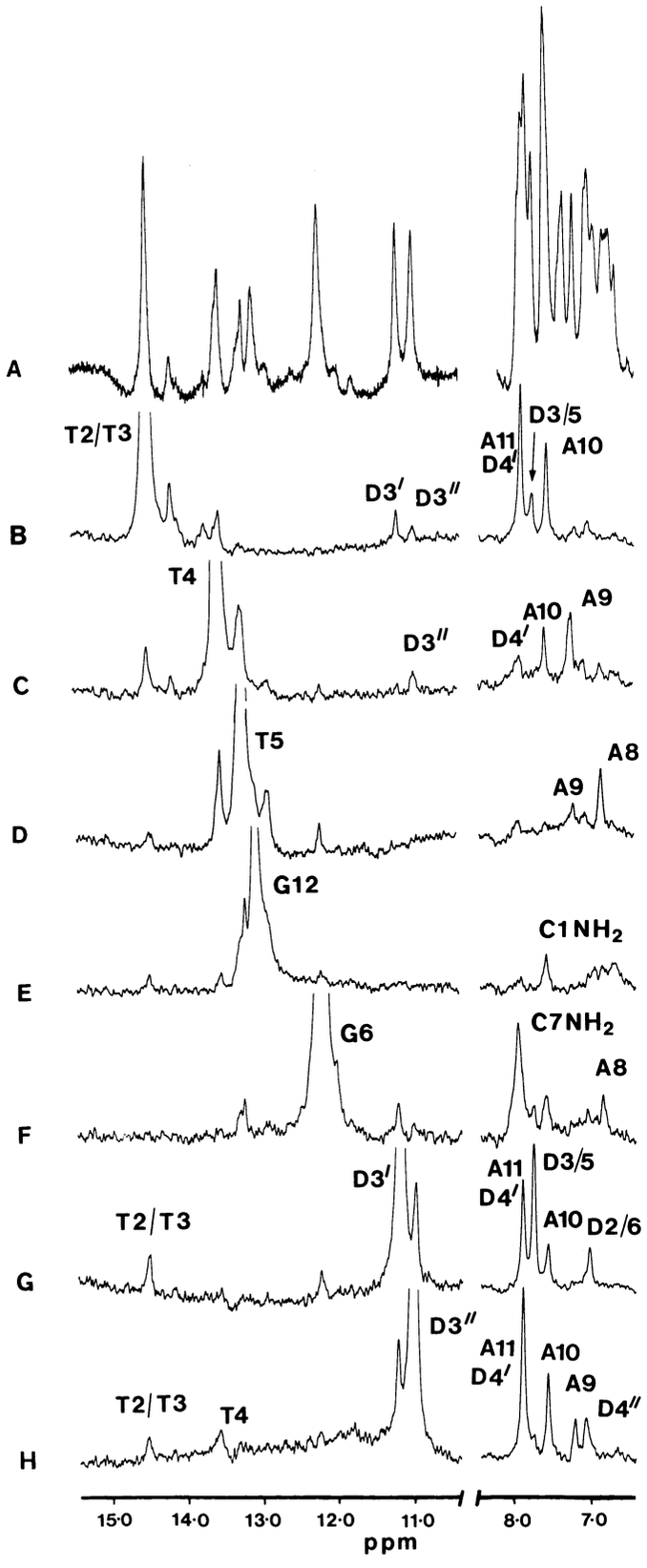

Figure 5. ^{1}H NMR spectrum (A) and NOE difference spectra (B)–(H) recorded in 90% H_2O/ 10% D_2O solution at 10°C. The 6.5–8.5 and 10.5–15.0 ppm regions of the spectra are illustrated. Difference spectra were obtained after 0.3 s saturation of specific resonances in the spectrum as follows; (B) T2H3/T3H3, (C) T4H3, (D) T5H3, (E) G12H1, (F) G6H1, (G) D3′ and (H) D3″. Prominent NOEs are labelled with imino proton resonances identified according to residue number, i.e. T2, T3, T4, T5, G6 and G12. The adenine H2s are labelled A8, A9, A10 and A11, while drug proton resonances are identified as elsewhere in the text.

and D3/5 and the DNA protons T2H1′, T3H1′ and A11H2. At the opposite end of the dye molecule D4″ (bz 2) and protons on the N-methylpiperazine ring show NOEs to A8H2 and A9H2 at the 5′-terminus of the adenine-tract. Between these two extremeties are the interactions of D3′ (bz 1) with T2H3, T3H3, A11H2 and A10H2, while D3″ (bz 2) is close in space to T3H3, T4H3, A9H2 and A10H2. This array of contacts between the protons on the concave surface of the drug molecules and DNA protons assosciated with the minor groove clearly orients Hoechst in this groove at the centre of the 5′-TTTT and 5′-AAAA sequences. The perturbations to the chemical shifts of the DNA resonances are particularly pronounced for the imino protons of T2 and T3, for the deoxyribose H1′ and adenine H2s of the T2-A11, T3-A10 and T4-A9 basepairs which is consistent with the aromatic benzimidazole and phenol rings of each Hoechst molecule spanning these basepairs in the minor groove. The N-methylpiperazine moieties point towards the centre of the duplex but are accommodated within the adenine-tract while the phenol rings are located at the 3′-ends of the A-T tracts close to the ends of the duplex. We observe no NOE effects between the N-methylpiperazine protons and any of the G6 or C7 nucleotide protons that might indicate overlap between this bulky portion of the drug molecule and the central G-C basepairs of the duplex.

DNA conformation

The directionality of the NOEs between the base H6/H8 and their own and 5′-flanking deoxyribose H1′, H2′ and H2″, but not those of the 3′-flanking sugar, demonstrates that the duplex retains its right-handed conformation in the complex. The pattern and intensity of intranucleotide NOEs (H1′-H2″ > H1′-H2′ and H2′-H6/8 > H1′-H6/8 ~ H3′-H6/8) are consistent with the sugar geometries lying broadly within the C2′-endo region of conformational space while the glycosidic bond angles fall in the standard anti range. Thus the complexed DNA takes on the general B-type DNA morphology but many other structural characteristics are identified that are reminiscent of adenine-tract structures studied in the crystalline state (23, 24). For example, strong interstrand NOEs are observed between adenine H2 and deoxyribose H1′ of the complementary nucleotide to the 5′-neighbouring side of the adenine. These NOEs are particularly intense for A11H2-T3H1′, A10H2-T4H1′, A9H2-T5H1′ (see Figure 4A) while NOEs between adjacent adenine H2s suggest that purine-purine stacking interactions are also an important feature of the duplex. Together the data indicate that the T2-A11, T3-A10 and T4-A9 basepairs, in particular, are highly propeller twisted to a degree comparable to that observed in the Hoechst-DNA crystal structures, namely 20–25° (12–14). Such a high degree of propeller twisting is thus consistent with the groove width of the A-T tract in the region of the dye molecule being especially narrow.

Overview of the structure

Many NOEs between protons on the complementary curved surfaces of Hoescht and the DNA minor groove have enabled us to locate the position and orientation of the dye molecules at the centre of the 5′-TTTT and 5′-AAAA sequences. A molecular graphics representation of the proposed structure of the complex is illustrated in Figure 7. Computer modelling studies indicate that the ends of the dye molecule reach to the edges of the G-C basepairs flanking the adenine-tract. The N-methylpiperazine moieties of the two symmetrically disposed drug molecules point towards the centre of the duplex but lie within the adenine-tract

Table I. ^{1}H chemical shift values (±0.01 ppm) for the 2:1 Hoechst-d(CTTTTGCAAAAG)$_2$ complex measured at 10°C.

DNA resonances							
Nucleotide	H1′	H2′/2″	H3′	H4′	H2/H5/CH$_3$	H6/H8	H1/H3
C1	5.60	2.04/2.36	4.36	3.81	5.66	7.63	–
T2	6.19	1.94/2.35	4.04	3.85	1.44	7.40	14.51
T3	5.12	1.55/1.91	4.29	3.68	1.35	7.12	14.51
T4	4.73	1.31/1.79	4.13	3.02	1.17	6.79	13.58
T5	4.23	0.91/1.12	4.12	nd	1.12	6.40	13.26
G6	5.40	2.22/2.24	4.03	3.77	–	7.45	12.29
C7	5.03	1.09/1.69	4.40	3.72	5.03	6.87	–
A8	5.07	2.48/2.51	4.70	4.01	6.90	7.96	–
A9	5.78	2.45/2.51	4.79	4.14	7.27	7.87	–
A10	5.10	1.76/2.22	4.32	nd	7.60	7.58	–
A11	4.76	1.61/1.97	4.20	3.36	7.92	7.26	–
G12	4.68	1.43/1.53	3.95	3.45	–	6.74	13.13
Hoechst resonances							
D2/6	7.06	D6′	7.65	D6″	6.84	D4‴(Me)	2.59
D3/5	7.79	D7′	7.88	D7″	7.42		
D3′	11.27	D3″	11.08	D2‴/6‴	2.99/3.95		
D4′	7.94	D4″	7.14	D3‴/5‴	2.99/3.42		

nd-not determined.

Table II. Intermolecular NOEs in the 2:1 Hoechst-d(CTTTTGCAAAAG)$_2$ complex.

Drug proton	DNA proton
D2/6	T2H3, T2H1′, T3H3, T3H1′, A11H2
D3/5	T3H1′, T3H4′, A11H2
D3′	T2H3, T3H3, A10H2, A11H2
D4′	T2H3, T3H1′, T3H3, T4H3, A9H2, A10H2
D3″	T2H3, T3H3, T4H3, A9H2, A10H2
D4″	A8H2, A9H2
D2‴/6‴	A8H2, A9H2
D3‴/5‴	A8H2, A9H2
D4‴(Me)	A8H2, A9H2

located close to the T5-A8 basepairs. Many van der Waals interactions are apparent between the inner face of the dye and the minor groove (see Table II), in particular the adenine H2s on the floor of the groove. These close contacts underlie the preference of Hoechst 33258 for the minor groove of A-T rich sequences rather than G-C rich. In the latter case severe steric clashes are encountered with the N2 amino group of guanine which would tend to push the Hoechst molecule out of the minor groove. In our model of the complex the H2s of A9, A10 and A11 lie close to the plane of the aromatic rings of the dye on the floor of the groove and this notion is confirmed by the observation of large downfield ring-current shifts of 0.55−0.82

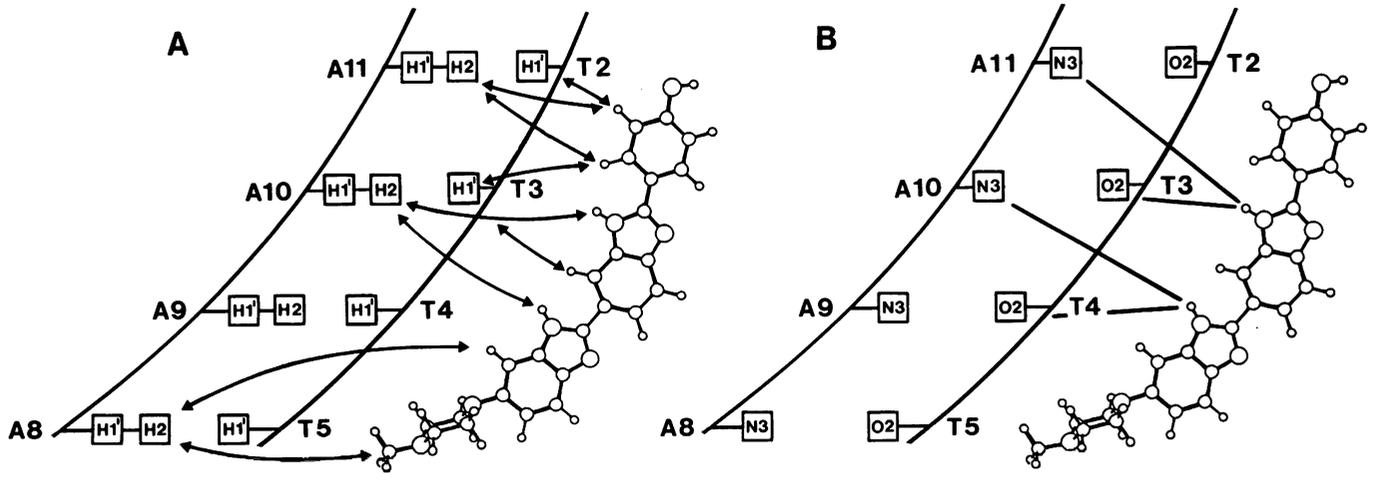

Figure 6. Schematic representation of Hoechst 33258 bound to the minor groove of the 5′-TTTT sequence. In (A) some of the NOEs are highlighted which determine the position and orientation of the Hoechst molecules within the minor groove. In (B) the intermolecular hydrogen bonding scheme is illustrated. Molecular modelling studies with an idealised B-DNA helical structure indicate that the benzimidazole D3′ is capable of forming bifurcated interactions with A11N3 and T3O2 while the benzimidazole D3″ hydrogen bonds in a similar manner but with A10N3 and T4O2. In our proposed model of the complex these distances fall within 3.5Å and are thus within acceptable hydrogen bonding limits.

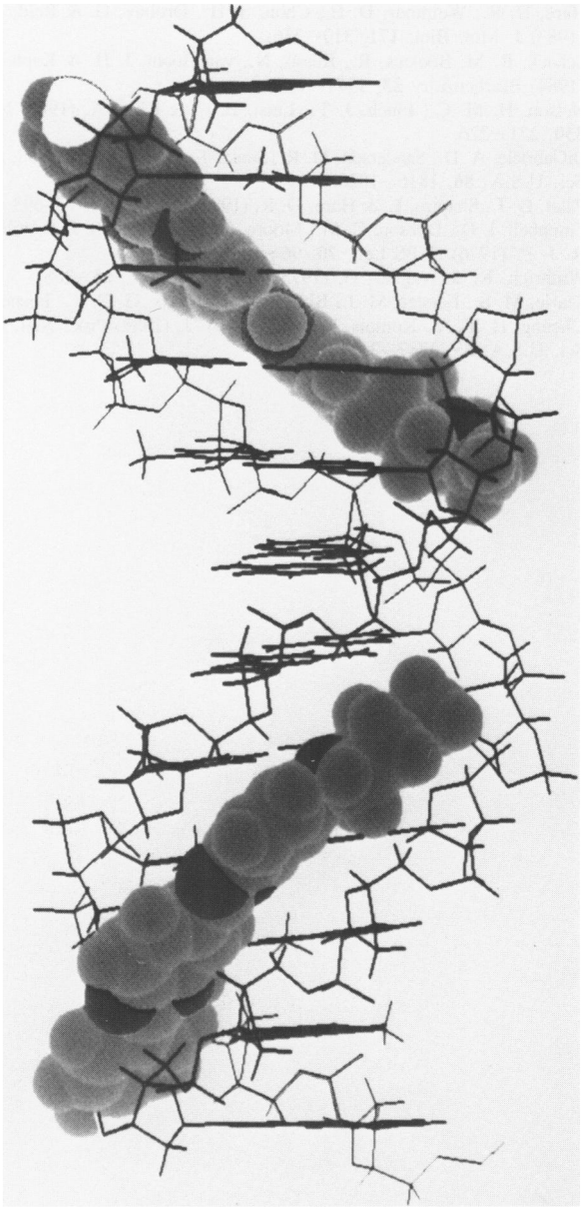

Figure 7. Molecular graphics representation of the Hoechst-d(CTTTTGCAAAAG)$_2$ complex with two molecules of Hoechst bound per duplex in symmetry related orientations.

ppm for these protons. Similarly large downfield shifts of ~1.0 ppm are observed for the imino protons of T2 and T3. Stabilizing van der Waals interactions are also evident from NOEs between drug protons and the deoxyribose H1's which form part of the walls of the binding site (see Table II). In this case we expect the sugar protons to be positioned above the plane of the aromatic rings of the dye which is consistent with the large upfield ring-current shifts of between 0.78 and 1.05 ppm observed for the H1's of T3, T4, A11 and G12. Large complexation shifts are also observed for the deoxyribose and base protons of T5 (see Figure 2B) which may be associated with electronic effects arising from the close proximity of the charge of the N-methylpiperazine rings to this nucleotide.

The NH protons D3′ (bz 1) and D3′′ (bz 2) present the opportunity for stabilizing hydrogen bonding interactions between the drug and the minor groove of the DNA, a notion consistent with their slow exchange rates and small temperature-dependence of their chemical shifts. Model-building studies, based upon the NOE data, ring-current effects and the high degree of propeller twisting observed for T2-A11, T3-A10 and T4-A9 are consistent with a system of bifurcated hydrogen bonds between the NH groups of the benzimidazole rings and the adenine N3 and thymine O2 atoms on the edges of the basepairs. The proposed interactions are represented schematically in Figure 6B and specifically involve bridging three-centre hydrogen bonds between D3′ (bz 1) and base A11N3 and T3O2, and from D3′′ (bz 2) to base A10N3 and T4O2. Electrostatic interactions also play an important role in stabilizing the complex. The minor groove of B-DNA in A-T rich regions has a particularly large negative charge potential and in the present complex stabilization of the positively charged N-methylpiperazine moiety will be greatest when these ends of the bound drug molecules are positioned at the centre of the helix rather than close to the ends. Thus electrostatic interactions are likely to be an important determinant of the orientation of the Hoechst molecules within this particular complex given that a similar set of stabilizing hydrogen bonding interactions are possible in either orientation.

Taken as a whole the data is consistent with the aromatic rings of the dye molecule being approximately coplanar with each other and fitting tightly within the minor groove orthogonal to the DNA basepairs. The high degree of propeller twisting observed for the T2-A11, T3-A10 and T4-A9 basepairs, which makes the minor groove within the adenine-tract particularly narrow, suggests that the van der Waals interactions between the drug molecule and the walls of the groove have a large stabilizing influence on the complex. In the reported crystal structures specific stabilizing interactions between drug and DNA involve the polarizable O4′ atoms of the deoxyribose rings. In the structure of Teng et al. (13) the average groove width within the AATT sequence, estimated from the distance between the O4′ atom of residue (n) on one strand and residue (n+2) on the complementary strand, is 6.45Å with the narrowest separation being only 6.02Å. This is compared with a width of 8.90Å for the flanking G-C basepairs. However, despite the apparent tight fit between the aromatic rings of the dye molecule and the minor groove of the DNA, dynamic features of the complex are also apparent from the NMR data. The presence of resonance averaging is apparent for both the D2/D6 and D3/D5 protons and is consistent with the environments on either side of the phenol rings being averaged by rapid ring-flipping motions about the C4-C2′ axis. Dynamics of this type are frequently observed for the tyrosine and phenylalanine sidechains within globular proteins (26, 27) and for small inhibitor molecules bound to enzymes (28). We were unable to freeze-out the ring-flipping motion within the accessible temperature range (>0°C) which suggests a lower limit on the rate of phenol ring rotation of >200 s^{-1} at 10°C, assuming a modest chemical shift difference between the two exchanging sites of 0.5 ppm. This rate is much faster than the rate of interconversion between free and bound forms of the duplex which we estimate to be <10 s^{-1} from the chemical exchange data. Thus dissociation of the drug from the complex, assuming this to be the rate limiting step in the chemical exchange process, cannot be the rate limiting factor for phenol ring-flipping. The available Hoechst-DNA crystal structure data indicate that intermolecular steric constraints prevent such a process from taking place and, therefore, the flipping motion

reflects a transient breathing of the structure as the rate limiting step. While the phenol ring is wedged within the narrow minor groove in the crystal structure, the orientation of the N-methylpiperazine ring appears to be somewhat disordered or conformationally flexible. Two equally populated radically different orientations are adopted in the structure reported by Pjura et al. (12) but a single orientation is observed by Teng et al. (13) where the N-methylpiperazine ring lies parallel to the benzimidazole rings. In our studies dynamic effects are also apparent for the resonances D2'''/6'''axial, D2'''/6''' equatorial, D3'''/D5''' axial and D3'''/D5''' equatorial of the N-methylpiperazine ring and here ring-flipping or free rotation also appears to be fast in the bound form of Hoechst as observed for the free ligand (unpublished results).

In conclusion, our data is consistent with Hoechst 33258 binding to the minor groove at the centre of the 5'-TTTT and 5'-AAAA tracts of the duplex $d(CTTTTGCAAAAG)_2$. We see no evidence for overlap with the flanking G-C basepairs as reported in two of the three crystal structures of Hoechst-DNA complexes (12, 13). However, we do not discount the influence of the flanking sequences on the binding affinity and orientation of the Hoechst molecule at specific sites as also concluded from the pattern and intensity of double-strand breaks induced by ^{125}I-labelled Hoechst with natural DNA (10, 11). A more detailed study of this and other Hoechst-DNA complexes using a number of structural refinement techniques will enable us to describe more fully distance and geometry relationships within these structures in solution.

ACKNOWLEDGEMENTS

K. J. E. is the grateful recipient of an Australian Postgraduate Research Award. We wish to thank Wendy Bicknell for providing technical assistance.

REFERENCES

1. Latt, S. A. & Wohlleb, J. C. (1975) Chromosoma **52**, 297–316.
2. Bontemps, J., Houssier, C. & Fredericq, E. (1975) Nucleic Acids Res. **2**, 971–984.
3. Stokke, T. & Steen, H. B. (1985) J. Histochem Cytochem. **33**, 333–338.
4. Raether, W. & Lammler, G. (1971) Annals of Tropical Medicine and Parasitology, **65**, 107–115.
5. Denham, D. A., Suswillo, R. R., Rogers, R., McGreevy, P. B. & Andrew, B. J. (1976) J. Helminthology **50**, 243–250.
6. Sreening data on NSC 322921 (Pibenzimol), National Cancer Institute, Bethesda, USA, 1983.
7. Marcus, M. & Sperling, K. (1979) Exp. Cell Res. **123**, 406–411.
8. Marcus, M., Goitein, R. & Gropp, A. (1979) Hum. Genet. **51**, 99–105.
9. Harshman, K. D. & Dervan, P. (1985) Nucleic Acids Res. **13**, 4825–4835.
10. Martin, R. F. & Holmes, N. (1983) Nature **302**, 452–454.
11. Murray, V. and Martin, R. F. (1988) J. Mol. Biol. **201**, 437–442.
12. Pjura, E. P., Grzeskowiak, K. and Dickerson, R. E. (1987) J. Mol. Biol. **197**, 257–271.
13. Teng, M.-K., Usman, N., Frederick. C. K. & Wang, A. H. -J. (1988) Nucleic Acids Res. **16**, 2671–2690.
14. Carrondo, M. A. A. F. de C. T., Coll, M., Aymami, J., Wang, A. H.-J., van der Marel, G. A., van Boom, J. H. and Rich, A. (1989) Biochemistry **28**,7849–7859.
15. Muller, L. & Ernst, R. R. (1979) Mol. Phys. **38**, 963–992.
16. Keeler, J. & Neuhaus, D. (1985) J. Magn. Reson. **63**, 454–473.
17. Clore, A. M., Kimber, B. J. & Gronenborn, A. M. (1983) J. Magn. Reson. **54**, 170–173.
18. Hore, P. J. (1983) J. Magn. Reson. **55**, 283–300.
19. Sanders, J. K. M. & Hunter, B. K. (1988) Modern NMR Spectroscopy, pp 210, Oxford University Press.
20. Clore, G. M. & Gronenborn, A. M. (1983) EMBO J. **2**, 2109–2115
21. Hare, D. R., Wemmer, D. E., Chon, S. H., Drobny, G. & Reid, B. R. (1983) J. Mol. Biol. **171**, 319–336.
22. Scheek, R. M, Boelens, R., Russo, N., van Boom, J. H. & Kaptein, R. (1984) Biochemistry **23**, 1371–1376.
23. Nelson, H. M. C., Finch, J. T., Luisi. B. F. & Klug, A. (1987) Nature **330**, 221–226.
24. DiGabriele, A. D., Sanderson, M. R., Steitz, T. A. (1989) Proc. Natl. Acad. Sci. U.S.A. **86**, 1816–1820.
25. Patel, D. J., Shapiro, L. & Hare, D. R. (1986) Biopolymers **25**, 693–706.
26. Campbell, I. D., Dobson, C. M., Moore, G. R., Perkins, S. J. & Williams, R. J. P. (1976) FEBS Lett. **70**, 96–100.
27. Wuthrich, K. & Wagner, G. (1975) FEBS Lett. **50**, 265–268.
28. Searle, M. S., Forster, M. J., Birdsall, B., Roberts, G. C. K., Feeney, J., Cheung, H. T. A., Kompis, I. & Geddes, A. J. (1988) Proc. Natl. Acad. Sci. U.S.A. **85**, 3787–3791.